Synthesis of Lithium Niobate Gels Using a Metal Alkoxide−Metal Nitrate Precursor

H. C. Zeng*,† and S. K. Tung‡

Department of Chemical Engineering and Department of Mechanical and Production Engineering, Faculty of Engineering, National University of Singapore, 10 Kent Ridge Crescent, Singapore 119260

Received March 20, 1996. Revised Manuscript Received June 27, 1996⊗

Gel material (Li:Nb = 1:1) of $LiNbO_3$ has been prepared from a novel precursor system, niobium(V) ethoxide−lithium nitrate. The resultant biphasic gel is calcined at various elevated temperatures and studied with FTIR/XRD/DTA/SEM methods for gel composition, crystallization, and morphological development. The progressive formation (crystallization) of $LiNbO_3$ is observed over the calcination temperature range 200−400 °C. It is found that grain growth and secondary recrystallization occur sequentially at higher temperatures. Retention behaviors of carbon-containing species and nitrate ions encapsulated in the gel matrix and a possible $LiNbO_3$ formation mechanism are also addressed.

Introduction

There is increasing in $LiNbO_3$ materials for use in optoelectronic applications.[1−14] Conventionally, $LiNbO_3$ and its related materials are prepared from high-temperature processes, such as single-crystal Czochralski growth,[8−10] capillary liquid epitaxial technique,[11] Stepanov growth,[12] laser-heated pedestal growth,[13] and preparation of $25Li_2O{\cdot}25Nb_2O_5{\cdot}50SiO_2$ glass.[14] Since $LiNbO_3$ is not a congruently melting compound, the chemical composition of the single crystals grown from the congruent melt is nonstoichiometric.[1,2] The degree of Li_2O deficiency in $LiNbO_3$ material determines the rates of solid-state diffusion within the crystal lattice as well as overall ferroelectric performance.[3−6] Due to the evaporation of the lithium or out-diffusion during material processing at high temperature,[7] the final chemical composition often varies from the originally desired one.

The solution sol−gel method opens a new avenue for low-temperature processing of $LiNbO_3$, especially for large-area thin-film fabrication.[15,16] In this regard, direct lithium loss in $LiNbO_3$ material is reduced by using this low-temperature technique. As a result, chemical compositions of $LiNbO_3$ are also more controllable. Over the past few years, $LiNbO_3$ crystalline materials have been prepared from all-metal-alkoxide type precursors, such as bialkoxide $Li(Nb(OC_2H_5)_6)$.[17−21] The techniques developed in these studies have shown great potential for future applications, as processing temperatures for the $LiNbO_3$ synthesis via sol−gel route can be significantly reduced.

To make full use of the technological merits of sol−gel-derived $LiNbO_3$ in fabrication of optoelectronic devices, it is necessary to search for new precursor systems,[15] to further lower both the processing temperature and preparation costs. As an effort to search for new routes of low-temperature $LiNbO_3$ synthesis, the current paper reports a study on preparation of $LiNbO_3$ gel material using a new precursor system: niobium ethoxide−lithium nitrate−2-propanol−acetylacetone−water.

Experimental Section

The $LiNbO_3$ gels were synthesized from the niobium(V) ethoxide ($Nb(OC_2H_5)_5$)−lithium nitrate ($LiNO_3$) system. The preparation procedure can be briefly summarized as follows: Niobium(V) ethoxide (Alfa Products) was diluted in 2-propanol solvent to give a sol with molar ratio of Nb(V) ethoxide to 2-propanol of 1:45. A chelating agent, acetylacetone (acac), was then added to the above solution with the molar ratio of acac to Nb(V) ethoxide [acac]/[Nb] = 1, to suppress rapid hydrolysis and control the reaction kinetics. The hydrolysis

* Corresponding author.
† Department of Chemical Engineering.
‡ Department of Mechanical and Production Engineering.
⊗ Abstract published in *Advance ACS Abstracts*, September 1, 1996.

(1) Carruthers, J. R.; Peterson, G. E.; Grasso, M.; Bridenbaugh, P. M. *J. Appl. Phys.* **1971**, *42*, 1846.
(2) Svaasand, L. O.; Eriksrud, M.; Nakken, G.; Grande, A. P. *J. Cryst. Growth* **1974**, *22*, 230.
(3) Gallagher, P. K.; O'Bryan, Jr., H. M. *J. Am. Ceram. Soc.* **1985**, *68*, 147.
(4) O'Bryan, H. M.; Gallagher, P. K.; Brandle, C. D. *J. Am. Ceram. Soc.* **1985**, *68*, 493.
(5) Guenais, B.; Baudet, M.; Minier, M.; LeCun, M. *Mater. Res. Bull.* **1981**, *16*, 643.
(6) Gallagher, P. K.; O'Bryan, Jr., H. M. *J. Am. Ceram. Soc.* **1988**, *71*, C-56.
(7) Birnie, III, D. P. *J. Mater. Sci.* **1993**, *28*, 302.
(8) Baumann, I.; Rudolph, P.; Krabe, D.; Schalge, R. *J. Cryst. Growth.* **1993**, *128*, 903.
(9) Furukawa, Y.; Sato, M.; Kitamura, K.; Nitanda, F. *J. Cryst. Growth* **1993**, *128*, 909.
(10) Kan, S.; Sakamoto, M.; Okano, Y.; Hoshikawa, K.; Fukuda, T. *J. Cryst. Growth* **1993**, *128*, 915.
(11) Fukuda, T.; Hirano, H. *J. Cryst. Growth* **1980**, *50*, 291.
(12) Red'kin, B. S.; Kurlov, V. N.; Tatarchenko, V. A. *J. Cryst. Growth* **1987**, *82*, 106.
(13) Luh, Y. S.; Feigelson, R. S.; Fejer, M. M.; Byer, R. L. *J. Cryst. Growth* **1986**, *78*, 135.
(14) Zeng, H. C.; Tanaka, K.; Hirao, K.; Soga, N. *J. Non-Cryst. Solids*, in press.
(15) Johnson, Jr., D. W. *Am. Ceram. Soc. Bull.* **1985**, *64*, 1597.
(16) Kazakos, A.; Komarneni, S.; Roy, R. *Mater. Lett.* **1990**, *9*, 405.
(17) Hirano, S.; Hayashi, T.; Nosaki, K.; Kato, K. *J. Am. Ceram. Soc.* **1989**, *72*, 707.
(18) Hirano, S.; Kato, K. *J. Non-Cryst. Solids* **1988**, *100*, 538.
(19) Yanovskaya, M. I.; Turevskaya, E. P.; Leonov, A. P.; Ivanov, S. A.; Kolganova, N. V.; Stefanovich, S. Yu.; Turova, N. Ya.; Venevtsev, Yu. N. *J. Mater. Sci.* **1988**, *23*, 395.
(20) Nazeri-Eshghi, A.; Kuang, A. X.; Mackenzie, J. D. *J. Mater. Sci.* **1990**, *25*, 3333.
(21) Joshi, V.; Mecartney, M. L. *J. Mater. Res.* **1993**, *8*, 2668.

S0897-4756(96)00197-4 CCC: $12.00

and incorporation of lithium were started simultaneously by adding the aqueous solution of lithium nitrate (10.488 M). Note that the aqueous lithium nitrate was added dropwise to the solution under magnetic stirring. When the cation ratio Li:Nb of the solution reached 1:1, the molar ratio of water to Nb(V) ethoxide would correspond to $[H_2O]/[Nb] = 3.56$ using the above 10.488 M lithium nitrate. The thus-prepared transparent solution was further stirred for another 1 h at room temperature and then transferred from the preparation beaker to Petri dishes, which were subsequently covered with pinholed sealing films to allow a slow interdiffusion between the solution vapor and ambient air, inside a fumehood. The gelation took place in about 3 h, indicated by a color change from the dark yellow transparent sol to a light-yellow opalescent but macroscopically homogeneous biphasic gel. The gel was continuously dried at room temperature inside the fumehood for 5 days, to generate a dry and light yellowish gel LN (i.e., $LiNbO_3$), which was still slightly opaque.

The pinholed cover was removed and LN gel was then heat-dried at 100 °C in an electric oven for 1 h to eliminate encapsulated water or possible adsorbed surface moisture. The thus-dried gel is designated as LN100 in the text, according to its chemical composition and calcination temperature. To study the $LiNbO_3$ formation upon calcination temperature, the LN100 gel was heat-treated at different temperatures, 200, 300, 400, 500, 600, 700, 800, 900, and 1000 °C, for 4 h with static air in a furnace (Carbolite). These heated gels were still in bulk form, though they cracked into smaller pieces after the calcination. The nomenclature of the resulting samples is similarly expressed in the text as LN200−LN1000.

The chemical composition and evolution of the $LiNbO_3$ gel series (LN100−LN1000) were examined with the Fourier transform infrared (FTIR) spectroscopic method (the KBr pellet technique) for its characteristic IR absorption bands. The FTIR spectra of the samples were recorded with a 4 cm^{-1} resolution on a computerized FTIR spectroscope (Shimadzu FTIR-8101). Typically, 1.2 mg of the finely ground gel sample was well mixed with 260 mg of dry spectroscopic grade KBr powder in a dry environment. The mixture was then pressed in a die to produce a transparent pellet. The spectrum background was corrected with a freshly prepared pure KBr pellet (260 mg) for each recorded spectrum. Forty scans were performed for each spectrum to obtain a good signal/noise ratio as previously described in the literature.[22,23] The crystallographic information on the above gel series were established by using X-ray diffraction (XRD) method. The diffraction intensity 2θ spectra were measured in a Philips PW 1729 with Cu Kα radiation ($\lambda = 1.5418$ Å) with a 2θ range of 5−70° at a scanning rate of 4°/min. Thermal behaviors of the $LiNbO_3$ gel series were studied with the differential thermal analysis (DTA). The DTA measurements were performed on a Shimazu DTA-50 in the nitrogen atmosphere with a gas flow rate of 20 mL/min. The temperature was scanned from room temperature to 1400 °C at a heating rate of 10 °C/min, and the sample weight in each DTA measurement was fixed at 30.0 mg. The microstructure and morphology of the gels LN100−LN1000 were examined on a JEOL JSM-T330A scanning electron microscope (SEM). Mean grain diameters of the crystallized gels (LN400−LN1000) were measured and averaged from magnified SEM micrographs [1.0 μm (real dimension) = 7.5 mm (photographic dimension)], and data were then analyzed.

Results

Chemical Constituent in Amorphous $LiNbO_3$ Gels. The FTIR spectrum evolution of the gels LN100−LN1000 is reported in Figure 1. For the low-temperature calcined samples LN100−LN500, absorption peaks at 1380 cm^{-1} are assigned to the nitrate ion NO_3^- remaining in the gels.[24] The round absorption bands located in the range 1360−1440 cm^{-1} of spectrum

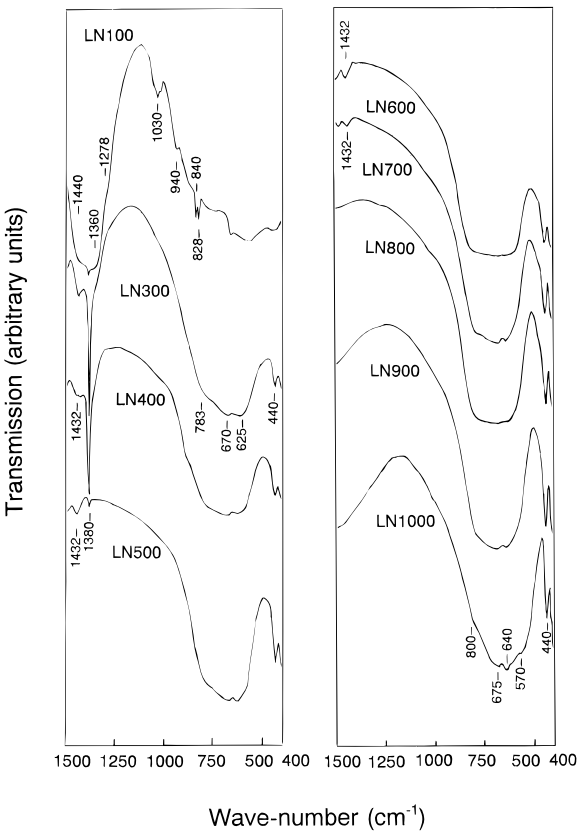

Figure 1. FTIR spectra recorded for the 100 °C heat-treated gel LN100 and its further calcined gel sample series LN300−LN1000 (300−1000 °C).

LN100 (similarly in LN200) can be attributed to CH_2 bending (1360 cm^{-1})[25,26] and CH_2 wagging (1440 cm^{-1}),[25] respectively, while the C−C skeletal stretching mode at 940 cm^{-1} can be clearly identified for the LN100 sample.[25,26] These hydrocarbon species reflect the fact that at 100 °C, certain organic compounds (backbones) are still retained or encapsulated in the amorphous gel LN100. In particular, the C−O mode at 1278 cm^{-1} [27] indicates that the solvent 2-propanol and hydrolysis products (alcohols) are still included in the gel at this temperature. The C═O vibration modes can be observed at 828, 840, and 1030 cm^{-1}, respectively,[28] from the spectrum LN100. These C═O bands are mainly originated from the chelating agent used in the experiments, as they are sensitive to the amount of acac added to the sols. It should be mentioned that the adding of acac molecules is essential during the sol preparation. Without them, the hydrolysis of $Nb(OC_2H_5)_5$ will occur vigorously, resulting in precipitates of niobium oxides. The presence of acac molecule in the LN100 sample suggests that a certain amount of central atom Nb may still be partially bound to the bidentate, although the gel LN100 can be thought as a mixture of amorphous

(22) Zeng, H. C.; Shi, S. *J. Non-Cryst. Solids* **1995**, *185*, 31.
(23) Zeng, H. C.; Lin, J.; Teo, W. K.; Loh, F. C.; Tan, K. L. *J. Non-Cryst. Solids* **1995**, *181*, 49.
(24) Monros, G.; Carda, J.; Tena, M. A.; Escribano, P.; Sales, M.; Alarcon, J. *J. Non-Cryst. Solids* **1992**, *147/148*, 588.
(25) Holland-Moritz, K. In: *Fourier Transform Infrared Characterization of Polymers*; Ishida, H., Ed.; Plenum Press: New York, 1987; p 190.
(26) George, B.; McIntype, P. *Infrared Spectroscopy*; John Wiley & Sons: Chichester, 1987; p 312.
(27) George, B.; McIntype, P. *Infrared Spectroscopy*; John Wiley & Sons: Chichester, 1987; p 327.
(28) Smith, A. L. *Applied Infrared Spectroscopy*; John Wiley & Sons: New York, 1979; p 288.
(29) Baran, E. J.; Botto, I. L.; Muto, F.; Kumada, N.; Kinomura, N. *J. Mater. Sci. Lett.* **1986**, *5*, 671.

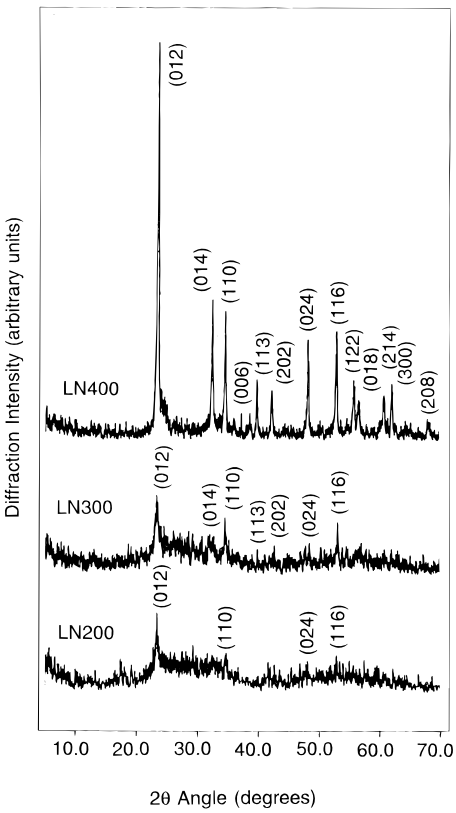

Figure 2. XRD spectra for low-temperature calcined gel samples LN200−LN400.

Nb_2O_5 and $LiNO_3$, i.e., a biphasic mixture (or nanocomposite).[15,16] This is further supported by the fact that no distinct $LiNbO_3$ IR absorptions are observed for the amorphous gel LN100 over the wavenumber range 400−800 cm^{-1}.[29]

Crystallization of $LiNbO_3$ Gels. The characteristic $LiNbO_3$ IR finger printing absorptions[29] over the wavenumber range 400−800 cm^{-1} appear observable in the spectrum of LN300, indicating the current gel has started to crystallize before 300 °C. In Figure 2, XRD results are shown for three low-temperature calcined gels LN200−LN400. As can be seen from spectrum LN200, the $LiNbO_3$ diffraction features, such as peaks (012) and (110), are observable at calcination temperatures as low as 200 °C. In line with the FTIR results, these diffraction intensities are getting pronounced when the temperature is increased to 300 °C. And at 400 °C, the XRD patten for $LiNbO_3$ has been fully developed.

It has been reported that there are four absorption modes observed for $LiNbO_3$ (ilmenite lattice) single crystal over the wavenumber range 400−800 cm^{-1} at 783, 630, 595, and 500 cm^{-1}, respectively.[29] In the current work, these four absorption modes can be detected in LN300 at 783, 670, 625, and 440 cm^{-1} and in LN1000 at 800, 675, 640, 570, and 440 cm^{-1} in Figure 1, respectively. The blue shifts observed in the LN1000 can be related to an increase in crystallinity from the gel LN300 to LN1000 or other subtle compositional changes upon heat treatment.[18] The new band at 570 cm^{-1} for LN1000 spectrum may be attributable to one of the expected optical modes but not been observed in ref 29, based on a factor group analysis for irreducible representation.[29]

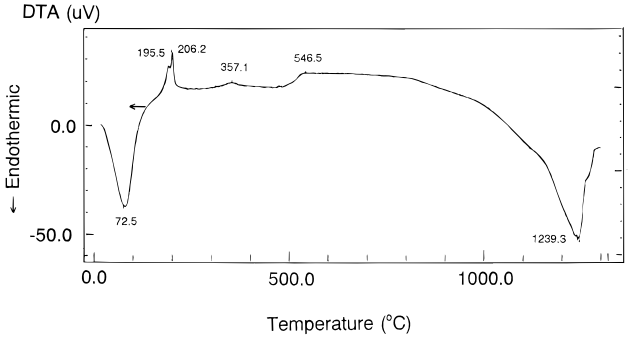

Figure 3. DTA analysis for the parent gel (as-prepared) LN over room temperature to 1300 °C, measured at 10 °C/min in N_2 atmosphere with a flow rate of 20.0 mL/min.

In agreement with the above FTIR/XRD observations, Figure 3 shows the formation $LiNbO_3$ from the amorphous gel LN during the thermal process of DTA measurement. The endothermic peak at 72.5 °C is attributed to the evaporation of organic compounds in the gel. The doublet peaks at 195.5 and 206.2 °C can be assigned to the organic radical combustion temperatures,[17] respectively, taking the FTIR/XRD evolution patterns into account. The endothermic band from 357.1 to 546.5 °C is attributable to chemical decomposition processes of NO_3^- and CO_3^{2-} groups, since FTIR result shows IR absorptions of these functional groups are significantly reduced over this temperature range (see Discussion). The temperature at 1239.3 °C corresponds nicely to the melting point (liquidus) of this *on-site* synthesized $LiNbO_3$.[1,2] The melting point obtained in DTA study indicates clearly the current gel series maintains well their chemical composition of $LiNbO_3$.

Microstructural Evolution of $LiNbO_3$ Gels. As shown in Figure 4a, the calcined gel LN300 shows laminate structures along the vertical direction. The cracks with preferential direction indicate an initial development of anisotropic nature (i.e., crystalline) of the gel at 300 °C. When calcination temperature reaches 400 °C, the temperature corresponding to full development of the $LiNbO_3$ phase, fine crystalline grains can be seen in LN400 (Figure 4b). In addition, small holes on the skin part can also be observed in the same sample. It is interesting to note that although the laminate form of LN400 gel is still maintained, the individual crystal grain is rather spherical, which is also true for other crystallized gels (LN500−LN900). Calculated from another SEM micrograph with a higher magnification, the average grain size of LN400 gel is 0.23 μm. Starting from 700 °C, grain growth becomes pronounced (Figure 4e,f). Compared with the gels LN500 and LN600, the gel densities of LN700 and LN800 are higher, judging from relative void space and number for these gels.

The above analyses for the grain size development versus firing temperature are summarized in Figure 5. As can be seen, there is a sharp increase in grain size in the 900−1000 °C region. This sudden rise in grain size can be described to the secondary recrystallization, which refers to rapid grain growth at the expense of a fine-grained matrix in ceramic science.[30] For example, it is evident that average $LiNbO_3$ grain size of the gel

(30) Kingery, W. D.; Bowen, H. K.; Uhlmann, D. R. *Introduction to Ceramics*; John Wiley & Sons: Singapore, 1991; p 448.

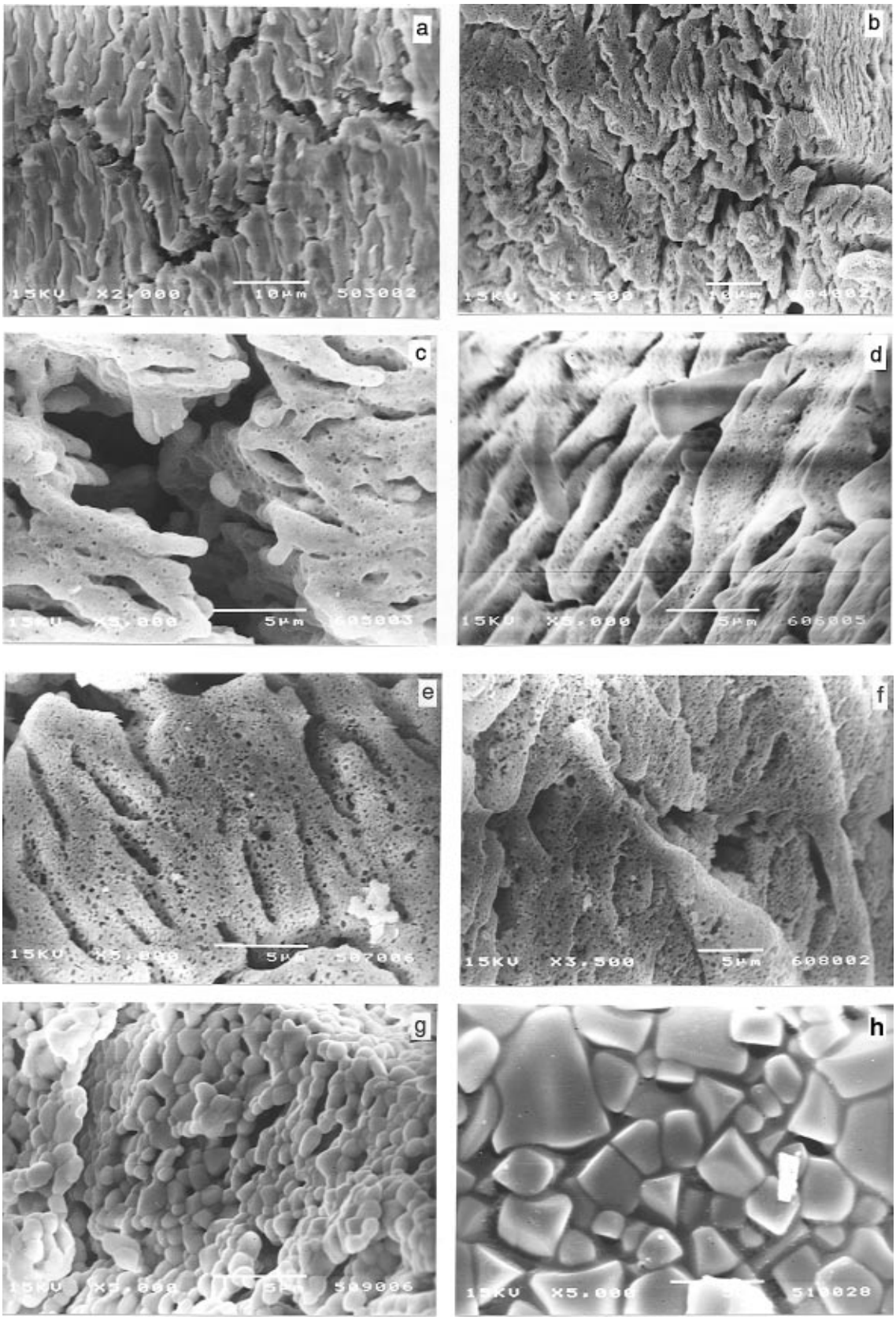

Figure 4. SEM micrographs of the calcined $LiNbO_3$ gel series: (a) LN300, (b) LN400, (c) LN500, (d) LN600, (e) LN700, (f) LN800, (g) LN900, and (h) LN1000. Bar lengths in (a) and (b) represent 10 μm, while in (c−h) stand for 5 μm.

LN900 (Figure 4g) is 0.97 μm, which is about 4 times greater than in the LN400, and the pore population is markedly reduced. When a firing temperature of 1000 °C is applied, the $LiNbO_3$ gel is highly densified (Figure 4h), showing a significant change in grain morphology. As can be seen from the micrograph of Figure 4h and 5, the average grain size of the LN1000 gel is about 3 times larger than that of the LN900. The chained ball-like grain morphology of the LN900 has been readily changed to the bucklike structure in LN1000. The formation of the bucklike LN1000 can be viewed as secondary recrystallization, which is formed at the

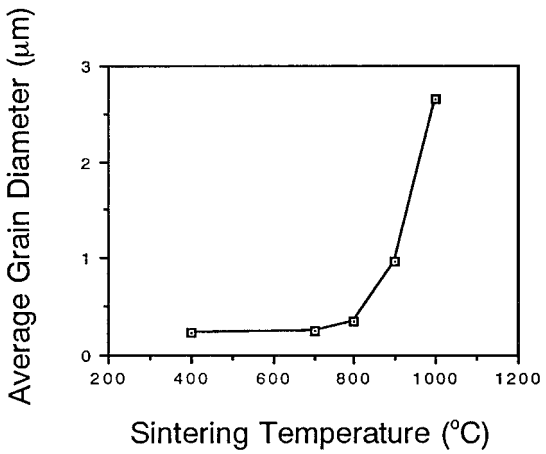

Figure 5. Average $LiNbO_3$ grain sizes after 4 h sintering at various temperatures, calculated from SEM micrographs with magnification of (1.0 μm = 7.5 mm photographic dimension). The line is drawn as a guide for the eye.

expense of smaller growing grains such as those in LN800 and LN900. The combination and thus multiplication of these smaller grains may offer an explanation.[30] As suggested by the smooth surface morphology for the gel LN1000, the $LiNbO_3$ material prepared may adopt the low-index grain surfaces during the rapid growth at this temperature. This explanation is in line with the observation that there is a significant mass relocation at this temperature, noting that the LN1000 sample also shows deep thermal etching of the grain boundaries.

Discussion

Depletions of Carbon- and Nitrogen-Containing Species. Since the sol−gel method involves using organometallic compounds and organic solvents, the carbon-containing species arising from reagents or hydrolysis products are often retained in the gel matrix in the form of anions after heat treatment.[22] For example, the CO_3^{2-} anion is commonly observed in most sol−gel-derived materials.[31] These anion species in the gel would directly affect conductivity of the material and thus optoelectronic performance. Using current material system, the nitrate ion is also introduced to the $LiNbO_3$ synthesis. There is thus a need to examine carbon/nitrogen retention behaviors in the gel matrix.

When the calcination temperature reaches 300 °C, organic functional groups disappear (LN300, Figure 1), suggesting an evaporation or decomposition of the included organic compounds occurs at this temperature. The depletion of the carbon containing species at this temperature is further indicated by the emerging of NO_3^- group at 1380 cm^{-1} [24] and characteristic absorption of CO_3^{2-} at 1432 cm^{-1}.[31] The latter, CO_3^{2-}, indicates that certain organic compounds have undergone chemical decomposition. Accompanied with the carbon/nitrogen depletions, the formation of $LiNbO_3$ can be observed over wavenumber range 400−800 cm^{-1} in the spectrum LN300.

From a dynamic view point, DTA result in Figure 3 is also in good agreement with the above FTIR observation. The broad endothermic band ranging from room temperature to around 180 °C is attributed to the depletion of the organic compounds. However, combining the DTA result with that of FTIR analysis, it is clear that there are actually several stages involved in this process. For example, simple physical desorption/evaporation occurs at a temperature below 100 °C (peaked at 72.5 °C), while elimination of the encapsulated or bound species indicated with various wavenumbers in the FTIR spectrum LN100 takes place at higher temperatures (100−180 °C). Shortly prior to the $LiNbO_3$ formation, any retained organic radicals are converted to CO_3^{2-} through combustion, which is recorded as the exothermic effects at 195.5 and 206.2 °C in DTA spectrum (Figure 3) and CO_3^{2-} absorption mode at 1432 cm^{-1} (LN300, Figure 1).[31] However, the decomposition products arising, such as CO_3^{2-} and NO_3^-, have to be depleted from the gel at a higher calcination temperature. For example, judging from peak intensity of 1380 cm^{-1} of FTIR spectra (Figure 1), it is recognized that the nitrate ion (NO_3^-) in the current gel series is continuously decomposed over the temperature range 300−500 °C. Similar observation is obtained for CO_3^{2-} (1432 cm^{-1}, Figure 1) species over this temperature range. On the basis of IR data, therefore, the endothermic effect at 357.1−546.7 °C of the DTA spectrum (Figure 3) can be assigned to the thermal decomposition of CO_3^{2-} and NO_3^- accordingly. Using a calcination temperature of 500 °C, the majority of the retained anions (CO_3^{2-} and NO_3^-) can be eliminated from the gel matrix; only a trace amount of the anions are observable at this temperature (LN500, Figure 1). It is important to point out that since the current gel series is in a large bulk form during the calcination, compared with dimensions in thin-film applications, mass-transport processes for the both anions in decomposition would be much more difficult. Taking this kinetic factor into consideration, it is believed that the temperature of 500 °C will be lowered further with a prolonged heat treatment time in the case of small spacial specimen dimension.

Back to the current experiment, among the CO_3^{2-} and NO_3^-, CO_3^{2-} is even more persisting in the gel matrix than NO_3^- after 500 °C. In fact, no NO_3^- can be detected in LN600 gel. But for CO_3^{2-}, a temperature of 800 °C is needed to completely eliminate the anion from the gel (LN800, Figure 1). As can be seen, anion NO_3^- introduced in the current case can be depleted at a temperature much lower than that of CO_3^{2-}. The addition of $LiNO_3$ does not introduce extra complications to $LiNbO_3$ synthesis, because most NO_3^- species can be eliminated from gel matrix over the similar temperature range for $LiNbO_3$ crystallization.

Possible Mechanism for $LiNbO_3$ Formation. The structure of precursor molecule $Nb(OC_2H_5)_5$ in solution has been suggested to be a dibridged dinuclear $Nb_2(OC_2H_5)_{10}$ complex.[20,32] With the introduction of acac, Li^+ and NO_3^- to the current precursor system, the dibridged structure will be certainly modified. Presumably, the chelation of acac to the $Nb_2(OC_2H_5)_{10}$ complex will weaken the bridging oxygen-coordinated niobium bond (O→Nb). The location of the cation/anion (Li^+/NO_3^-) pair in the solution is another interesting topic. Due to the electrostatic charge effect, furthermore, there

(31) Colomban, Ph.; Bruneton, E. *J. Non-Cryst. Solids* **1992**, *147, 148*, 201.

(32) Yogo, T.; Kikuta, K.; Ito, Y.; Hirano, S. *J. Am. Ceram. Soc.* **1995**, *78*, 2175.

must be some chemistry between the host complex [$Nb_2(OC_2H_5)_{10}$−acac] and the ion pair. These will be the subjects for our future study.

When the above-mentioned precursor complex undergoes the hydrolysis and gelation, amorphous Nb_2O_5 phase results. It is our belief that the Li^+/NO_3^- ion pair, together with other polar product compounds as a second phase, are dispersed well within the Nb_2O_5 framework due to self-charge-compensation. As proposed in the previous two sections, after the hydrolysis/gelation, the LN (and similarly LN100) gel can be described as a nanocomposite precursor consisting of the amorphous Nb_2O_5 and Li_2O (or Li^+/NO_3^- before the nitrate salt decomposition) microbiphasic system. Although the two phases (and thus Li and Nb) may not be mixed as inherently as that in the case of all metal alkoxides,[15,16] the contact area between the phases is certainly much larger than that in the ceramic powder synthesis. And indeed, the current material system crystallizes at a much lower temperature than those of conventional $Li_2O-Nb_2O_5$ powder synthesis. In view of the results of FTIR/XRD/DTA investigations, the full development of $LiNbO_3$ phase would be anticipated in the calcination temperature range 300−400 °C. Nevertheless, since there is no distinct exothermic effect observed in DTA over this range (300−400 °C, Figure 3), the crystallization/formation of $LiNbO_3$ should be regarded to be a diffusion-controlled continuous process. Considering the amorphous Nb_2O_5 phase alone, it is noted that Nb−O−Nb network has already built in atomic scale during the sol−gel preparation.[15,16] The formation of $LiNbO_3$ phase in the current precursor system, however, requires a diffusion of Li^+ ions into the Nb_2O_5 matrix; diffusion activation energy is thus anticipated. As the exothermic effects at 195.5 and 206.2 °C (Figure 3) can be assigned to the oxidation of organic groups in the Nb_2O_5 matrix,[17] it is our belief that these exothermic effects of organic radical combustion may further promote the formation/crystallization of $LiNbO_3$, driving Li^+ ions into Nb_2O_5 framework thermally. This speculation is validated by the observation of $LiNbO_3$ XRD features in low-temperature calcined gels LN200-LN300 (Figure 2), where localized combustion heat seems to be responsible for this early $LiNbO_3$ formation.

Using the double alkoxide, such as $Li(Nb(OC_2H_5)_6)$, crystallization temperatures of stoichiometric $LiNbO_3$ fibers, powders, and thin films have been reported to be 450, 350−700 °C, respectively,[17−21] although a lower temperature of 250 °C has also been achieved for $LiNbO_3$ thin film on Si(100) surface.[18] Evidenced in our FTIR/XRD/DTA investigations, the crystallization temperature of $LiNbO_3$ for the current material system is comparable to those using all-alkoxide precursors. The synthesis of sol−gel-derived $LiNbO_3$ from this new precursor system therefore seems to be a viable route to obtain $LiNbO_3$ at a relatively low fabrication temperature and low cost.

Conclusion

In summary, $LiNbO_3$ gel materials with Li:Nb = 1:1 atomic ratio have been prepared from the new precursor system: niobium ethoxide−lithium nitrate−2-propanol−acetylacetone−water. By using FTIR/XRD/DTA/SEM techniques, it is found that a continuous formation of $LiNbO_3$ occurs over the calcination temperature range 200−400 °C; the temperature of which is comparable to those reported in the literature using all alkoxide precursors. The grain growth and secondary recrystallization are also observed for the gels at higher temperatures sequentially. The retention behaviours of anion species encapsulated in the gel matrix have been discussed, and the possible mechanism of $LiNbO_3$ formation has also been proposed for this biphasic precursor system.

Acknowledgment. The authors gratefully acknowledge the research fundings supported by the National Science and Technology Board of Singapore and National University of Singapore and the technical assistance provided by Ms. W. C. Ng.

CM960197N